https://doi.org/10.52131/jee.2025.0601.0057

*i*RASD Journal of Energy & Environment

Volume 6, Number 1, 2025, Pages 92 - 111

Journal Homepage:
https://journals.internationalrasd.org/index.php/jee

TRNSYS-Based Performance Study of Solar-Assisted Single-Effect Absorption Cooling in Peshawar, Pakistan

Abid Hussain[1], Asnaf Aziz[2], Afzal Khan[3], Nadeem Ur Rehman[4], Hamza Pervez[5], Altaf Husain[6]

[1] Lab Engineer, Department of Mechanical Engineering, University of Engineering and Technology Peshawar, Pakistan. Email: abidhussain@uetpeshawar.edu.pk
[2] Lecturer, Department of Mechanical Engineering, University of Engineering and Technology Peshawar, Pakistan. Email: asnafaziz@uetpeshawar.edu.pk
[3] Professor, Department of Mechanical Engineering, University of Engineering and Technology Peshawar, Pakistan. Email: afzalkhan@uetpeshawar.edu.pk
[4] Lab Engineer, Department of Mechanical Engineering, University of Engineering and Technology Peshawar, Pakistan. Email: nadeem.rehman@uetpeshawar.edu.pk
[5] Graduated Student, Department of Mechanical Engineering, University of Engineering and Technology Peshawar, Pakistan. Email: 21pwmec5096@uetpeshawar.edu.pk
[6] Graduated Student, Department of Mechanical Engineering, University of Engineering and Technology Peshawar, Pakistan. Email: 21pwmec5020@uetpeshawar.edu.pk

ARTICLE INFO

Article History:

Received: Feburary 26, 2025
Revised: June 04, 2025
Accepted: June 06, 2025
Available Online: June 08, 2025

Keywords:

Climate Adjustment
Eco-friendly Development
Efficiency of Collector
Energy Economizing
Pakistan
Renewable Energy
Solar Fraction
Transient Simulation
TRNSYS 18

JEL Classification Codes:

Q42, Q54, Q57

Funding:

This research received no specific grant from any funding agency in the public, commercial, or not-for-profit sectors.

ABSTRACT

This study presents a detailed techno-economic and thermal performance evaluation of a solar-assisted absorption cooling system optimized for the climatic conditions of Peshawar, Pakistan. Through dynamic simulations conducted over the summer season (May to September), the performance of key subsystems, including the solar collector array, auxiliary heater, thermal storage, and absorption chiller, was analyzed. Simulation results demonstrate that the system successfully maintains the chilled water outlet temperature at 7°C, with consistent cooling water and hot water temperatures of 28°C and 95°C, respectively. The system exhibits steady-state flow rates of 650 kg/hr (cooling), confirming effective hydraulic control. Under variable load conditions, the auxiliary heater responded through frequent pulsed flow patterns, achieving peak flow rates up to 49,000 kg/hr without compromising outlet temperature. Parametric analysis revealed that the optimal tilt angle for solar collectors is approximately 15°, maximizing solar fraction (SF) for both flat plate collectors (FPC) and evacuated tube collectors (ETC). For ETCs, primary energy savings (PES) ($f_{sav,shc}$) of 0.49 were achieved using 560 m² of collector area and 14.9 m³ of thermal storage. The ideal storage volume was found to be 25 L/m², beyond which auxiliary energy consumption increased. Seasonal simulations revealed strong diurnal variations in cooling demand, peaking around 1.6 MW, while heating loads remained negligible, reinforcing the cooling-dominated nature of the operational period. The system's average seasonal solar collector efficiency was calculated at 0.188 for FPCs and 0.52 for ETCs, underscoring the superior thermal performance of ETCs at higher driving temperatures (111°C). A minimum of 400 m² collector area was required to achieve 50% primary energy savings. These findings validate the hybrid solar-auxiliary configuration's suitability for high-demand cooling applications in arid climates and offer design insights for optimizing collector area, storage volume, and control strategies. The results not only optimize system design for local climatic conditions but also underscore the broader potential of solar cooling technologies to mitigate urban heat,

lower electricity demand, and enhance energy resilience in developing regions. These perceptions provide valuable guidance for renewable infrastructure planning and policy constitution across the same climatic regions.

Corresponding Author's Email: abidhussain@uetpeshawar.edu.pk
Citation: Hussain, A., Aziz, A., Khan, A., Rehman, N. U., Pervez, H., & Husain, A. (2025). TRNSYS-Based Performance Study of Solar-Assisted Single-Effect Absorption Cooling in Peshawar, Pakistan. *IRASD Journal of Energy & Environment*, *6*(1), 92–111. https://doi.org/10.52131/jee.2025.0601.0057

1. Introduction

The growing worldwide need for air conditioning is becoming a remarkable issue for sustainable planning of energy, especially in areas such as Peshawar, Pakistan, where utmost summer temperatures drive a great increase in cooling requirements. Speed urbanization, increase in population, and developing lifestyle standards have broadly strengthen the pressure on normal energy infrastructures (Perwez, Sohail, Hassan, & Zia, 2015). Conventional vapor compression cooling systems, which are steadily dependent on generation of electricity from fossil fuels, give substantially to emissions of greenhouse gas and environmental humiliation. As a result, the demand to develop and accept environmentally manageable and energy-efficient cooling technologies has never been most critical. In feedback to these issues, solar-powered cooling systems have appear as a feasible and sustainable replacement. These systems tackle solar thermal energy, plentiful in sun-rich zones just like as Peshawar, to power cooling technologies that can remarkably decrease dependence on usual fuels (Bhatkar, Kriplani, & Awari, 2013). Among the accessible solar cooling technologies, absorption systems, especially those using a lithium bromide–water (LiBr–H_2O) working fluid, provide considerable applications. These systems appoint a refrigeration cycle operated thermally, which allows them to work successfully using sources of low-grade heat, just like solar collectors. Compared to other thermally operated systems like absorption cooling units, absorption chillers usually provide a greater coefficient of performance (COP), making them more satisfactory for medium- to large-scale applications, involving institutional buildings (Ren, Qian, Yao, Gan, & Zhang, 2019).

However, the incorporation of solar energy into cooling systems shows various technical and operational challenges. Important points among them are the irregular nature of solar radiation, system design upgradation, thermal storage incorporation, and the operation of auxiliary energy consumption (Gang, Wang, Xiao, & Gao, 2016). A well-designed system must not only increase utilization of solar energy but also decrease losses from pumps, control units, and auxiliary heating components. Here, the latest simulation tools such as TRNSYS has become essential for the design and analysis of solar-powered cooling systems (Shesho, 2014). These principles allow researchers to conduct transient simulations over a large periods, allowing for accurate evaluation of system behavior under true climatic conditions without the need for expensive experimental setups (Darema, 2005). Regarding the capacity of simulation tools, a determined challenge lies in bridging the gap between simulated and real system performance (Hays & Singer, 2012). Real-world working environments, such as fluctuating solar irradiance, changes in room temperature, and load profiles usually introduce complications that are difficult to observe fully in simulation environments (Tress et al., 2019). Therefore, accurate modelling and validation using local climate data are necessary to verify that simulation results are representative of real-world performance, especially in diverse climatic zones just like that of Peshawar.

The current research work focuses on the modelling, simulation, and performance analysis of a solar-powered single-effect absorption cooling system adapted for the hot and dry atmosphere of Peshawar. The system use ETCs because of their high thermal efficiency under diffuse radiation conditions, combined with a thermal energy storage tank that justify a continuous and stable supply of thermal energy to the absorption chiller. The cooling system is designed to encounter a maximum load of 177 kW for an educational institution, with emphasis placed on optimizing key system parameters including surface area, tilt

angle of collector, and storage tank capacity. This work distinguishes itself by exploring the interplay between solar collector performances, storage dynamics, and cooling efficiency using TRNSYS. It evaluates key performance indicators such as collector efficiency, solar fraction, and PES under the specific environ-mental conditions of Peshawar. Through systematic parametric analysis and scenario comparisons, the study seeks to identify an optimal system configuration that maximizes energy savings, reduces environmental impact, and enhances the feasibility of large-scale deployment of solar-assisted cool-ing systems in Pakistan. By offering a detailed and dynamic performance assessment of a LiBr–H_2O based absorption cooling system, this study contributes to the broader goal of promoting clean and sustainable energy technologies for cooling applications. The insights gained from this research are expected to aid designers, engineers, and policymakers in making informed decisions for future implementations of solar-powered cooling systems across similar climatic regions. While numerous studies have explored solar-assisted cooling systems in hot climates, our work distinctly advances the field through its integration of real climatic data for Peshawar, which has not been extensively investigated in prior literature. Previous studies in Pakistan, such as those by Asim (2016), have examined SF and energy savings under generalized or idealized conditions. In contrast, our use of a TRNSYS-based simulation incorporating hourly weather data, building load profiles, and operational control dynamics offers a more realistic depiction of system behavior throughout the summer season. Moreover, our focused analysis on collector tilt angle (optimized at 15°), thermal storage sizing (expressed in L/m²), and the distinction between FPC and ETC configurations presents novel insights that have not been comprehensively explored in the regional context. This detailed parametric analysis highlights optimal design configurations that ensure maximum energy savings with minimal auxiliary energy input, which is especially critical for areas with high solar irradiance but limited energy infrastructure. These unique aspects collectively establish the methodological and contextual novelty of our study in the domain of solar-assisted cooling for arid climates. The specific objectives of the study are as follows:

The summary of Literature review is given in Table 1.

Table 1
Summary of Relevant Simulation Studies on Solar-Assisted Cooling

Study	Location / Climate	Tool Used	System Type	Key Focus	Findings
Khan et al. (2018)	Karachi, Pakistan (Hot & Humid)	TRNSYS	LiBr-H_2O Absorption Cooling	SF & energy savings under variable solar input	Peak SF of 0.58; emphasized collector size and pump control
El-Shazly et al. (2020)	Cairo, Egypt (Arid)	TRNSYS	Single-effect Absorption	Collector type and operating temp influence on COP	ETC outperformed FPC in annual performance; max COP ≈ 0.74
Ren et al. (2019)	Tehran, Iran (Dry & Sunny)	Simulink	Solar-Assisted Cooling + Storage	Dynamic modeling of cooling loads and chiller behavior	Emphasized control logic and storage volume on stability
Shesho (2014)	Baghdad, Iraq (Hot-Dry)	TRNSYS	LiBr-H_2O Absorption Cooling	Energy savings estimation under fixed solar radiation input	Average COP ≈ 0.7; demonstrated ~50% primary energy saving
Zahedi et al. (2024)*	Lahore, Pakistan (Semi-arid)	TRNSYS	Hybrid Cooling with Thermal Storage	Optimization of tank size and collector area	Identified optimal ratio of 25 L/m²; peak fsav,shc = 0.52
Current Study	Peshawar, Pakistan (Hot-Arid)	TRNSYS	ETC + LiBr-H_2O + Storage	Real climate data, collector tilt, and parametric optimization	$f_{sav,shc} \geq 0.50$ at 400 m² collector; Tilt angle = 15° optimal

1.1. Research Objectives

1. To develop a TRNSYS-based simulation model of a single-effect LiBr–H_2O absorption chiller integrated with ETC and thermal storage.
2. To evaluate the system's thermal and hydraulic performance under real climatic conditions of Peshawar during the summer season.
3. To analyze the effect of key design parameters—such as collector tilt angle, storage volume, and collector area on SF and primary energy savings.
4. To compare the performance of FPC and ETC in terms of efficiency and suitability for high-temperature cooling.
5. To assess the seasonal variation in cooling demand and identify strategies to optimize auxiliary energy use and thermal storage operation.

1.2. Guiding Research Questions

1. How effectively can a solar-assisted absorption cooling system maintain required thermal set points under Peshawar's summer climate?
2. What is the optimal collector tilt angle and thermal storage volume that maximize SF and minimize auxiliary energy use?
3. How do the thermal efficiencies and energy savings of ETC and FPC compare in this application?
4. What are the system's dynamic responses to diurnal cooling load variations, and how can performance be optimized to enhance energy efficiency?

2. Materials and Methods

This section outlines the configuration of the solar-assisted absorption cooling system, the simulation environment, and the methodology adopted for system modelling, performance evaluation, and optimization.

2.1. System Description

The proposed solar-assisted cooling system is designed to meet the peak cooling demand of 177 kW for an educational building located in Peshawar, Pakistan (34.0151°N, 71.5805°E), a region known for its extended summer season and high levels of solar irradiance. The system combine various important components to ensure reliable and efficient operation. At the basic of the design are ETCs, which work as the initially heat source by converting diffuse and direct solar radiation, into thermal energy. ETCs are especially fit for high-temperature atmosphere due to their excellent performance under such conditions. The thermal energy is stored in a Hot Water Tank, which works as a buffer between the absorption chiller and the solar field. This storage tank enables thermal load shifting and supports continuous working during time of reduced solar availability. The cooling process is operated by a Single-Effect Lithium Bromide–Water (LiBr–H_2O) Absorption Chiller, which utilizes the thermal energy from the storage tank in lieu of electricity, making it a more eco-friendly alternative to normal vapor compression systems. To ensure the reliability of the system, an Auxiliary Heater (or back-up boiler) is included to supply additional thermal energy when solar input is not enough, thereby maintaining compatible cooling output. The system's working is operated by a Cooling Load Profile developed depend on typical patterns and local atmosphere data, allowing it to efficiently meet the cooling requirement related to the Peshawar atmosphere.

2.2. Simulation Tool

The transient simulation was conducted using TRNSYS 18, a modular software globally used for simulating the performance of renewable energy systems with respect to time. Key components used from the TRNSYS library are shown in Table 2:

Table 2
Key Components used in TRNSYS 18

Type	Name	Function
Type 24	Online Plotter	Displays simulation results in real-time graphical form during the simulation. Useful for debugging and understanding dynamic behavior.
Type 25c	Printer (Formatted Output)	Outputs selected variables to a text file in a formatted layout for later analysis. Type 25c allows labeled and customized data output.
Equa	Equation Block	A user-defined block where custom algebraic or logical equations are written. Used to perform calculations, conditional statements, and control logic between components.
Type 65d	Online Plotter (Multiple Curves)	Plots multiple outputs simultaneously during simulation. Type 65d offers enhanced plotting features compared to Type 24.
Type 71	Integrator	Integrates an input over time to compute cumulative values, such as energy or volume totals. Commonly used for calculating total energy delivered or used.
Type 4a	Hot Water Storage Tank (Stratified)	Models a stratified thermal storage tank, important for systems involving solar thermal energy. Accounts for temperature layers and mixing.
Type 99	User-Defined External Component	A placeholder or interface for integrating custom code (e.g., Fortran, DLLs) not provided by standard TRNSYS libraries.
Type 114	Weather Data Processor (TMY2/TMY3)	Processes typical meteorological year (TMY) weather data to provide ambient temperature, solar radiation, wind speed, etc., to the system.
Type 682	Solar Collector (Evacuated Tube)	Models ETC with thermal characteristics and optical efficiency. Suitable for high-efficiency solar thermal systems.
Type 107	LiBr–H_2O Absorption Chiller	Simulates the performance of a single-effect absorption chiller using lithium bromide and water as working fluids. Heat-driven, typically used with solar systems.
Type 108	Auxiliary Heater / Boiler	Models an auxiliary heating source (usually gas/electric) to provide backup thermal energy when solar is insufficient.
Type 686	Pump (Variable Speed or Fixed)	Simulates fluid flow through the system. Controls flow rates and power consumption, essential for moving heat transfer fluid between components.
Type 700	Solar Radiation Processor	Calculates the solar radiation on tilted surfaces from horizontal radiation data using Perez or isotropic models.
Type 14h	Time-Dependent Forcing Function	Allows defining a load or schedule (e.g., hourly cooling demand). Type 14h supports high-resolution data (hourly, sub-hourly). Useful for replicating building cooling loads or user-defined profiles.

The methodological approach of the study was structured into several sequential steps to ensure a comprehensive and systematic analysis of the solar-assisted cooling system. The process began with site selection and climate data collection, focusing on Peshawar, where Typical Meteorological Year Meteonorm data was utilized to obtain accurate climate and solar radiation inputs. Seasonal trends in temperature, solar irradiance, and humidity were carefully analyzed to understand their influence on system performance throughout the year. Following this, system design and component sizing were carried out. Initial estimates for important parameters such as area of collector, tilt angle of collector, and volume of storage tank were derived from established guidelines in the literature. These initial values were then adjusted through repeated simulations to set with the specific site conditions and load requirements. The cooling load capacity was showed by a fixed chiller of 177 kW, which was selected to meet the maximum cooling demand. The next step included development of model using TRNSYS, a transient simulation tool widely used for modelling of energy system. In TRNSYS, all system parts were adjusted in a portable configuration, allowing for clear relationship and data flow between them. Control

policy were executed using differential controllers, which activated pumps depend on temperature differentials, therefore confirming efficient heat transfer and working stability. The system's performance was evaluated using important performance indicators, including efficiency of collector, SF, which shows the proportion of thermal energy provided by solar sources and PES, presenting the decrease in fossil fuel use due to solar combination. A comprehensive parametric analysis was performed to assess the impact of changing system parameters on performance. This included evaluating the effects of different collector types ETC vs. FPC, collector areas ranging from 50 to 150 m², storage tank volumes ranging from 2 to 8 m³, and tilt angles from 15° to 45°. The main aim was to point out the optimal configuration that would provide the maximum efficiency while minimizing the dependency on auxiliary energy sources. Finally, in the data analysis phase, simulation outputs were exported to Excel, where comparative performance analysis was performed. Graphs were generated to visualize trends in collector efficiency, variations in solar fraction, and monthly energy savings, facilitating a clear understanding of the system's behaviour under different conditions. The parameters used in the simulation are given in Table 3.

Table 3
Parameters used in the simulation TRNSYS 18

Peak cooling load	**177 kW**
Set point temperature of chilled water	6.7 ℃
Inlet temperature of cooling water	15 ℃
Minimum temperature needed for the operation of chiller generator	112 ℃
Flowrate of hot water between the storage tank and the chiller	46.57 m^3/hr
Flowrate of chilled water between the chiller and the building load	43.65 m^3/hr
Flowrate of cooling water the heat rejection of chiller	145.74 m^3/hr
Specific heat capacity of water	4.2 kJ/kg. K

2.3. Solar Collector

Types 71 and 1b refer to ETC and FPC, respectively. The thermal efficiency equation (Assilzadeh, Kalogirou, Ali, & Sopian, 2005) describes how these solar collectors perform:

$$\eta = a_o - a_1 \frac{\triangle T}{G} - a_2 \frac{(\triangle T)^2}{G} \quad (1)$$

In this context, the parameter a_o represents the optical efficiency of the solar collector, while a_1 and a_2 correspond to the first-order and second-order heat loss coefficients, respectively. These coefficients are critical in determining the thermal performance of solar collectors. According to the ASHRAE standard (Rojas, Beermann, Klein, & Reindl, 2008), G is defined as the total global solar irradiance incident on the surface of the collector, and the temperature difference (ΔT) is calculated as the difference between the ambient room temperature and the temperature of the fluid entering the collector. On the other hand, the European standard (Rojas et al., 2008) provides a little different approach, explaining ΔT as the difference between the room temperature and the average temperature of the heat transfer fluid flowing through the collector. These definitions can guide to slight changes in performance evaluation based on the standard used. The performance characteristics of FPC are further explained by Klein (1988) and ETC by Khan, Badar, Talha, Khan, and Butt (2018), which shows the respective values of a_o, a_1, and a_2 under changing fluid flow rates, supplying a comparative basis for analyzing efficiency of collector and heat loss behavior under various working conditions.

2.4. Auxiliary Boiler Working and Estimation of Energy Consumption

In the TRNSYS simulation model, Type 700 is used to indicate an auxiliary steam boiler that adjust the heating process by increasing the temperature of the working fluid to match the working requirements of the absorption chiller. This component becomes active when solar energy is not enough to obtained the require thermal level. The boiler's operation is controlled by predefined combustion characteristics and thermal efficiency settings, which are utilized to find its energy consumption (Rojas et al., 2008).

$$Q_{boiler} = m_f C_{pf}(T_o - T_1) \quad (2)$$

Where, C_{pf} and m_f represent the specific heat capacity and mass flow rate of the working fluid passing through the absorption chiller and storage tank, respectively.

2.5. Storage Tank

Type 4a, a part from the standard TRNSYS library, is used for the simulation of a stratified thermal storage tank with uniform heat losses. It use a multi-node modelling approach, where the tank is split into a particular number of nodes in this case, nine to express the thermal stratification and transient energy exchanges happening in the tank. Each node conducts an individual energy balance with respect to time, allowing the model to track temperature gradients and thermal behavior with more precision (El Hassani, Charai, Moussaoui, & Mezrhab, 2021). In the system configuration, the top node is nominated to provide heated fluid to the generator of the absorption chiller, guaranteed that the greatest-temperature fluid is used for cooling. For the time being, the bottom node is connected to the solar collector, undergoing the incoming solar-heated fluid and contributing to the stratification process. A constant heat loss coefficient of 0.829 W/m²·K is provided uniformly across all nodes during the simulations, ensuring consistent thermal loss modelling and providing accurate judgement of the tank's thermal performance.

2.6. Absorption Chiller

Type 107, component of the TRNSYS standard component library, is used to simulate a single-effect absorption chiller. This chiller operates by regenerating the refrigerant in the generator through the ap-plication of hot water, in conjunction with a working fluid mixture comprising a refrigerant and ab-sorbent. Its performance is controlled via an external performance file, which uses key input parameters to determine operational behavior. These inputs include the inlet temperature of the cooling water ($T_{cw,i}$), the generator's hot water inlet temperature ($T_{g,i}$), and the desired chilled water temperature set point ($T_{chw,set}$). While the default model is configured for a maximum cooling capacity of 1494 kW and a coefficient of performance (COP) of 0.53, the current study adapts this chiller to function under a reduced load of 177 kW to match the system's design requirements. This adjustment guarantees that the simulation accurately shows the scaled-down operation related to the building's cooling requirement. Utilizing this configuration, the model determines the required thermal input (Q_{hw}) the quantity of hot water energy that must be provided to the generator. This thermal input is matched through an integration of heat obtained from the solar collector system and, when necessary, provided by the auxiliary boiler, as shown in Klein (1988).

$$Q_{hw} = \frac{Rated\ Capacity}{Rated\ COP} f_{Design\ Eenergy\ Input} \quad (3)$$

The $f_{\text{Design Energy Input}}$ represents the fraction of the absorption chiller's rated energy input needed to match the current cooling demand. This factor guarantees that the system works efficiently under partial load conditions by scaling the energy input as compare to the full capacity of the chiller. It is critical to account for variations in the temperature of the incoming hot water, which can vary from 108 °C to 116 °C based on the system conditions. For simulation purposes, a lowest generator inlet temperature ($T_{g,i}$) of 111 °C is accepted to guarantee reliable working and accurate performance assessment of the absorption chiller. To find the actual cooling effect provided, the heat extracted from the chilled water loop ($Q_{chilled}$) is determined. This value shows the important cooling output of the system and is calculated using a defined relationship that integrates factors just like the mass flow rate of the chilled water, its specific heat capacity, and the temperature difference across the chiller. This calculation is necessary for judgement whether the thermal input from the solar collector and/or auxiliary boiler is enough to match the cooling load (Klein, 1988).

$$Q_{chilled} = m_{chw} C_{P\,chw}(T_{chw,in} - T_{chw,set}) \quad (4)$$

Where, $C_{P\ chw}$ and m_{chw} indicate the specific heat capacity and mass flow rate of chilled water, respectively. At every time step of the simulation, the total heat rejected by the cooling tower (Q_{cw}) is calculated by conducting a extensive energy balance on the absorption chiller. This energy balance explains all the thermal interactions in the system, securing correct representation of heat flows. In a single-effect absorption chiller, the energy balance is controlled by the principle that the sum of the thermal energy input from the hot water (Q_{hw}) and the cooling effect provided to the chilled water loop ($Q_{chilled}$) must equal the total heat rejected to the cooling water loop (Q_{cw}). Mathematically, this is expressed as Klein (1988):

$$Q_{cw} = Q_{hw} + Q_{chilled} + Q_{aux} \quad (5)$$

The term Q_{aux} represents the energy used by the solution pump, controllers, and other auxiliary components. When the chiller is operating, the assumed model the peak rated value for Q_{aux}, irrespective of whether it is running at full load or partial load (Hang & Qu, 2010).

2.7. Load Calculation

Type 682, a component available in the TRNSYS standard library, is a custom-defined load simulator designed to represent a constant or variable thermal load, which can be applied for either heating or cooling applications. It calculates the fluid outlet temperature based on the specified thermal load, making it a versatile tool for dynamic energy modeling. In the current work, Type 682 is used specifically to simulate the cooling load changes of a building. It acts as a synthetic load generator, producing cooling demand profiles by referencing a user-defined peak cooling load. This component incorporates hourly variations driven by daylight availability as well as seasonal patterns, thus mimicking realistic fluctuations in building cooling demand over time.

2.8. Weather Data

Type 99 is a TRNSYS component responsible for managing and importing weather data into the simulation model. In the current research, the weather information is stored in a user-prepared text file containing important meteorological parameters specific to Peshawar, Pakistan, including its geographic coordinates at latitude of 34.0151°N, and longitude of 71.5805°E. The modelling of solar cooling absorption unit using TRNSYS 18 is presented in Figure 1.

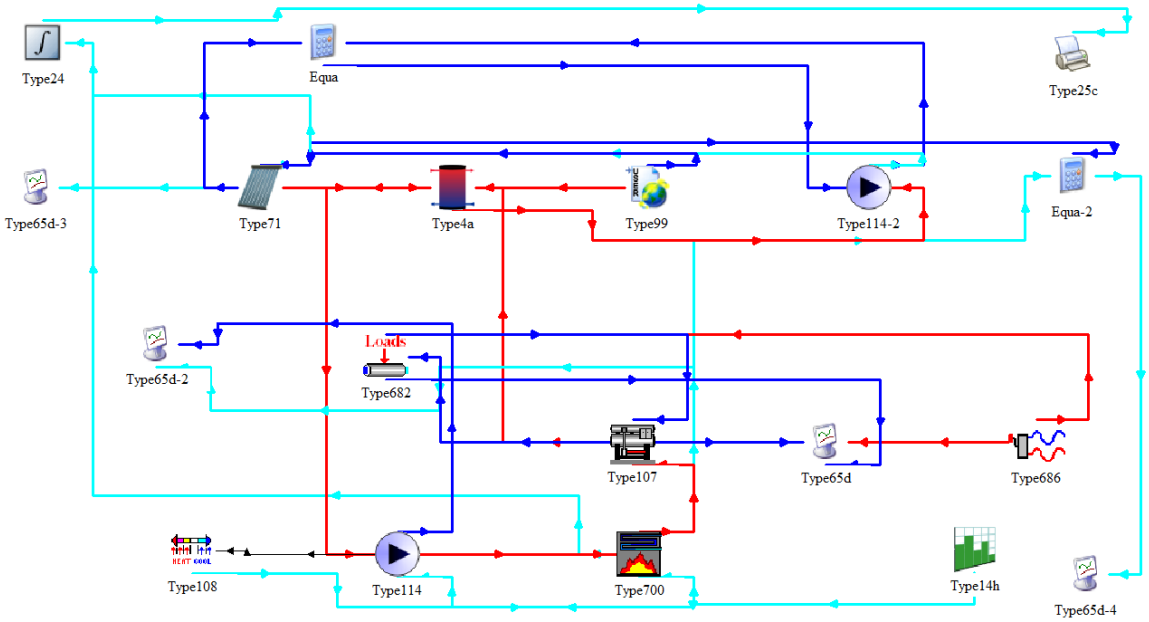

Figure 1: Modelling of solar cooling single effect absorption unit using TRNSYS 18

2.9. Important Assumption Used During Modelling of the System

To ensure real and representative simulation results, the following important assumptions and parameter were applied:

1. Cooling Load (177 kW)

The system was designed to achieve the maximum cooling demand of an educational building in Peshawar. The value of 177 kW was obtained from typical building cooling loads described in regional studies and energy audits (e.g., Khan et al. (2018)). This value also matches with TRNSYS simulation modules for institutional buildings under full occupancy during maximum summer hours.

2. Area of Solar Collector (400–1650 m²)

The collector area range was selected depended on prior parametric studies in similar atmospheric zones (Zahedi et al. (2024); Ren et al. (2019)). The lower value (400 m²) sows the minimum area required to obtain SF ≥ 0.49 using ETCs, while the upper value allows evaluation of oversizing effects on storage and auxiliary demand.

3. Collector Tilt Angles (5°–30°)

Tilt angles were changed to judge optimal solar gain during summer months. A tilt angle of 15° was found to yield the highest SF in line with findings by Klein (1988) and confirmed by simulation results. This range also complies with solar installation guidelines in low-latitude regions.

4. Weather Data

Hourly weather data (solar irradiance, ambient temperature, humidity) for Peshawar was sourced from Meteonorm and formatted into TRNSYS-compatible TMY2 files. This ensures that simulations reflect actual local climate conditions.

5. Thermal Storage Sizing (10–100 m³)

Storage volumes were selected based on the collector area-to-storage ratio of 25–60 L/m², as recommended in solar cooling design guidelines and validated in our parametric analysis. Oversizing effects were assessed for PES and auxiliary heater behavior.

6. Auxiliary Heater Operation

The auxiliary heater (Type 700) was programmed to maintain a setpoint of 95°C, engaging only when solar input was insufficient. Cycling behavior was observed under a differential temperature control strategy with minimal hysteresis.

7. Control Strategy

Flow rates and component operations were governed by TRNSYS control blocks using fixed values or step functions derived from a synthetic cooling demand profile (Type 682). This ensures quasi-steady simulation under defined load conditions.

8. System Losses

Heat losses in piping and tank insulation were incorporated using standard TRNSYS loss coefficients (U-values between 1.0–1.5 W/m²K). Pump parasitic loads were assumed at 2–5% of thermal input, consistent with system design norms.
The flowchart for methods and materials is shown in Figure 2

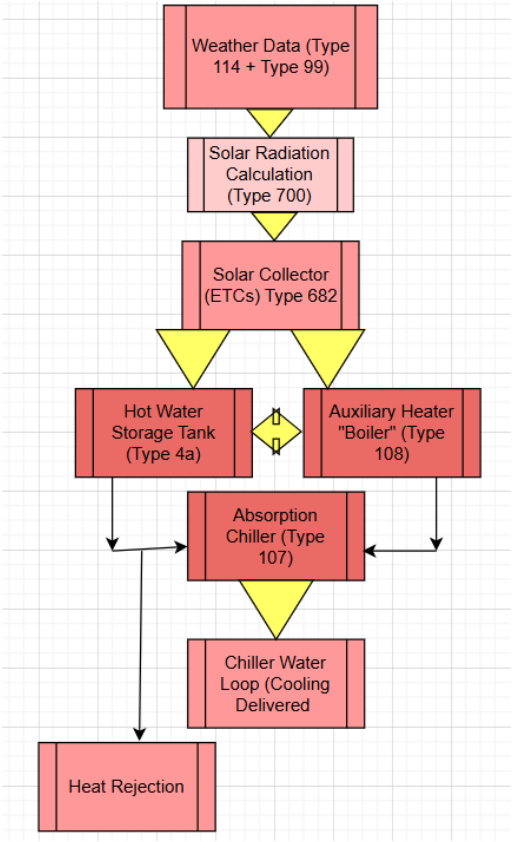

Figure 2: Solar-Assisted Absorption Cooling System

It is important to note that the simulation assumes certain idealized conditions for simplicity and model stability. These include a constant chiller COP throughout operation, ideal control strategies without sensor lag or actuator delays, and the exclusion of maintenance downtime or system degradation over time. While these assumptions facilitate parametric analysis and baseline performance evaluation, they may lead to slight overestimation of system efficiency in real-world scenarios. Future work should incorporate dynamic COP values based on load and temperature conditions, realistic control algorithms, and reliability modeling to capture operational disruptions and enhance the applicability of simulation outcomes to field implementations.

3. Results and Discussion

3.1. Steady State Analysis

Figure 3 presents the simulation results of the thermal and flow behaviour of the absorption cooling system over a selected operational period. The graph illustrates the outlet temperatures of three key fluid streams—chilled water, cooling water, and hot water—along with the corresponding flow rates on both the cooling and heating sides of the system. The outlet temperature of the hot water ($T_{\_out\_hot}$), depicted in purple, remains steady around 95°C throughout the simulation period. This consistent temperature indicates reliable thermal input to the absorption chiller's generator, suggesting that the combined solar and auxiliary heating system is able to meet the required thermal conditions without interruption. The outlet temperature of the cooling water ($T_{\_out\_cool}$), shown in blue, remains almost at 28 ℃, representing effective heat rejection through the cooling tower. For the time being, the outlet temperature of the chilled water ($T_{\_out\_chilled}$), indicated in red, is stable at around 7 ℃, which meets well with typical chilled water supply temperatures used in HVAC applications. This guarantees that the chiller maintains its cooling set point efficiently under the given load conditions.

On the secondary axis, the cooling flow rate (orange) and the heating flow rate (green) are indicated. Both flow rates appear to be constant over the observed time period,

with values close to 900 kg/hr for heating and 650 kg/hr for cooling. The absence of fluctuations suggests that the system operates under steady-state or quasi-steady conditions, likely due to the use of a synthetic load profile (Type 682) and constant input values during this segment of the simulation. The flat trends across all parameters in this interval indicate that the system is operating under a stable load scenario, which may correspond to a controlled test period within the broader simulation timeline. This behaviour confirms the model's ability to sustain operational requirements without thermal or hydraulic instability. The stable chilled water outlet temperature also verifies that the absorption chiller is performing within its intended de-sign capacity of 177 kW. Such results are essential for validating system design choices, particularly regarding component sizing and control strategy. The steady temperatures and flow rates reflect proper stratification within the thermal storage (Type 4a) and consistent auxiliary heat support (Type 700), contributing to the overall stability of the system.

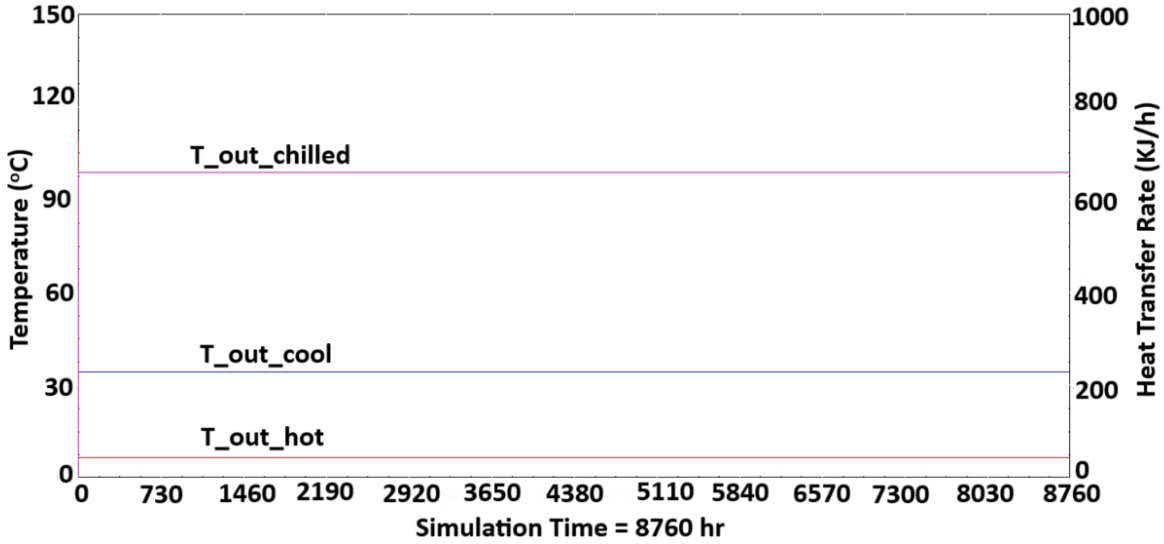

Figure 3: Temperature and Flow Rate Profiles of Hot, Cooling, and Chilled Water Streams during Steady-State Operation

3.2. Auxiliary System Behavior

Figure 4 displays the thermal and hydraulic behavior of the auxiliary heating system and circulation pump during a defined simulation period. The graph represents the temperature profiles of the pump outlet (TPump) and auxiliary heat source (TAux) alongside the heating fluid flow rates on the secondary axis. The temperature output from the auxiliary heater (TAux), shown in blue, remains consistently around 95°C, indicating that the auxiliary boiler reliably maintains the set point temperature required to supplement solar heating. The TPump trace, indicated in red, mirrors this behavior and confirms that the heated fluid is effectively circulated without significant temperature drop, reflecting minimal thermal losses in the piping or during transit. The heating flow rate, represented in magenta and yellow, shows a repetitive pulsed pattern, with frequent and sharp fluctuations occurring throughout the timeline. The maximum flow rate appears to reach approximately 49,000 kg/hr, which is notably high and likely represents transient or peak load operation when the auxiliary boiler is fully engaged. This pulsating flow behavior suggests that the auxiliary system is operating in an intermittent mode, likely controlled by a differential temperature controller. The activation occurs whenever the solar contribution is insufficient to meet the thermal demand, causing the boiler to cycle on and off frequently. The yellow and magenta flow rate lines overlap almost completely, indicating strong consistency in both actual and target flow rates within the heating loop. The periodic nature of flow pulses, while maintaining a constant temperature, indicates that thermal demand is being met efficiently, but also points to potential room for optimization. Frequent cycling may lead to mechanical wear on the pump and associated control components. Adjusting the hysteresis settings or incorporating thermal storage buffering could smooth these

fluctuations. This behavior also reflects the auxiliary system's responsiveness and the control strategy's sensitivity to demand variation a desirable characteristic for systems relying on hybrid solar-auxiliary configurations to maintain temperature thresholds essential for absorption chiller operation.

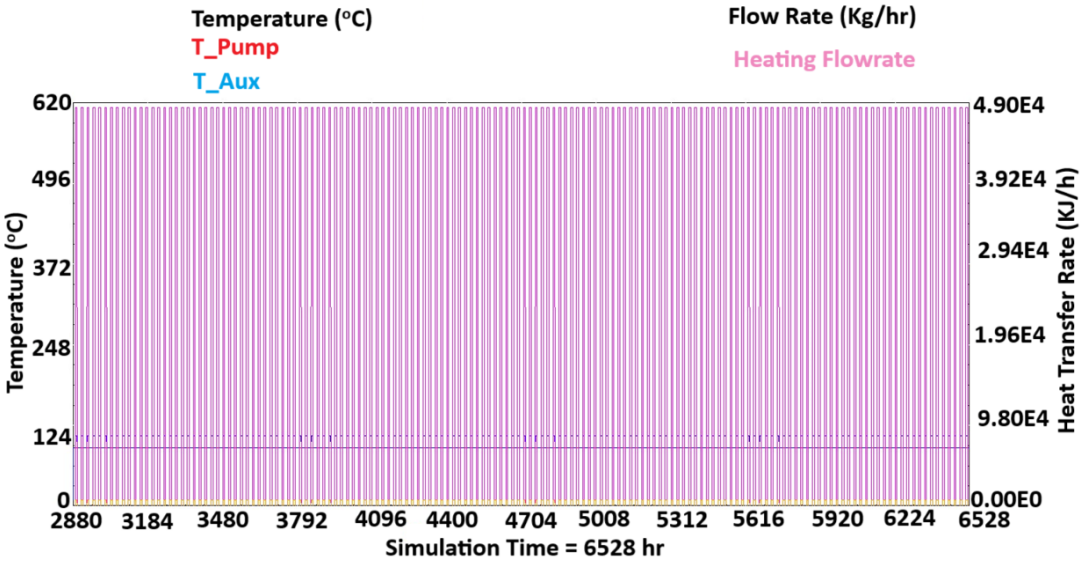

Figure 4: Temperature and Flow Rate Characteristics of the Auxiliary Heating System and Circulation Pump during Dynamic Operation

3.3. Dynamic Operation

Figure 5 presents the temporal variation of system temperatures and thermal loads over a selected simulation period spanning from 2880 to 6528 hours. The graph displays the outlet temperatures of the chilled, cool, and hot water circuits, along with the inlet temperature of the chilled water loop. At the same time, the heating and cooling loads are covered to check the transient response of the system under changing thermal requirments. The outlet temperature of chilled water ($T_{out\_chilled,\ red}$) remains consistently low across the simulation period, ahowing effective temperature regulation at the cooling side. The outlet temperature of cool water ($T_{out\_cool,\ blue}$) indicates a modest fluctuation, balancing around a mid-range value, while the outlet temperature of hot water ($T_{out\_hot,\ magenta}$) indicates a stepped profile, suggestive of a discrete control policy or stepped heating equipment operation. The inlet temperature of chilled water ($T_{in\_chilled,\ orange}$) indicates a great fluctuation, which mirrors the changes in cooling requirements and is likely effected by external thermal loads. This temperature behavior locates to a responsive chilled water loop system, adapting to varying thermal inputs while keeping supply conditions within operational bounds. The stepped design in hot water temperatures shows cyclic operation, possibly aligned with a scheduled or demand-based heating policy. The cooling (green) and heating (cyan) load pattern indicates clear temporal profile. The cooling load shows remarkable variability, with daily peaks and troughs showing substantial variation, compatible with building occupancy and external weather conditions. The maximum cooling load values are in the range of 1.6 MW, indicating high instantaneous demand, while the heating load remains relatively low throughout the simulation duration. The high frequency and amplitude of cooling demand show that the cooling system works near its capacity during peak time, potentially emphasizing system parts if not appropriately managed. The consistent presence of load spikes implies rapid fluctuations in thermal conditions, which might necessitate improved load-smoothing or energy storage strategies. The combined analysis of temperature and load trends suggests that the system is predominantly in a cooling-dominated regime during the analyzed period. This could correspond to summer or high external heat gain conditions. The thermal system appears to operate effectively within this envelope, but the significant cooling peaks may indicate opportunities for performance optimization—such as variable-speed control, predictive cooling strategies, or enhanced insulation to reduce demand spikes. Moreover, the limited heating load further suggests

seasonal variation, where heating demand is negligible compared to cooling requirements. This asymmetry emphasizes the importance of designing HVAC systems tailored to the predominant operational mode and integrating demand-side management to ensure energy-efficient operation.

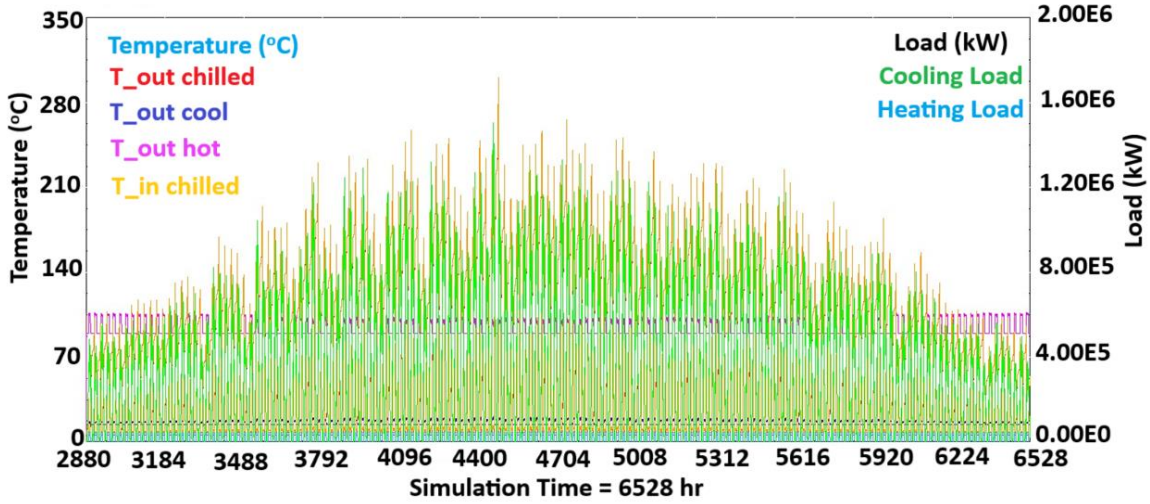

Figure 5: Dynamic Behavior of System Temperatures and HVAC Loads during Simulation

3.4. Parametric Analysis

Simulations were conducted throughout the summer season, (May to September). In the lack of experimental data from a genuine system for direct validation, the model's accuracy was assessed by comparing the trends in select simulation findings to those in previously published research. Figure 6 illustrates how the tilt angle of the collector affects the solar fraction. It shows that the solar percentage peaks at a tilt angle of the collector of around 15° for both ETC and FPC, while the area of collector, mass flow rate, and storage capacity remain constant. This observation, that tilt angle of collector influences solar fraction, is consistent with those published by Klein (1988) and Khan et al. (2018).

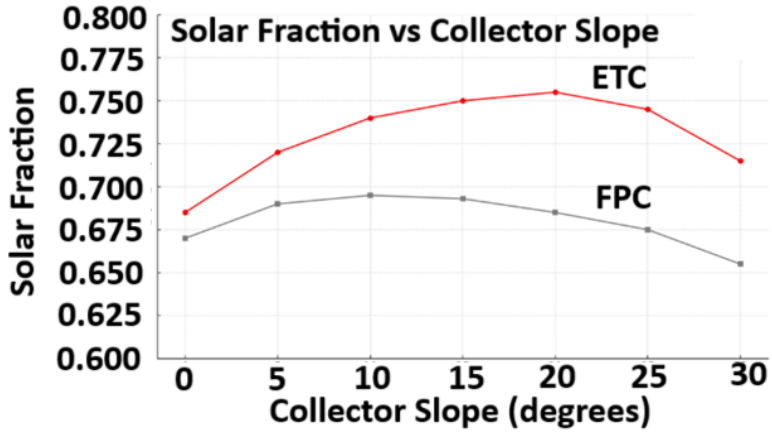

Figure 6: Variation of SF with Collector Slope for FPC and ETC

Figure 7 depicts that how the size of thermal storage affects fractional PES ($f_{sav,shc}$) in FPC areas. The graph indicates that when tank size increases, $f_{sav,shc}$ initially rises but then decreases. With a collector area of 1650 m², a $f_{sav,shc}$ of 0.50 is achieved when the thermal storage size is 60 m³ (29 L/m²).

Figure 8 depicts the link between volume of thermal storage and PES ($f_{sav,shc}$) for various sizes of ETCs. The observed trend is similar to that in Figure 9; however, the higher thermal efficiency of ETCs results in a significantly smaller ideal storage size. For a main

energy savings of at least 0.49, an ETC area of 560 m² and a storage volume of 14.9 m³ are needed. To save the same amount of primary energy, area of solar collector and capacity of thermal storage can be lowered to 400 m² and 10 m³ (equal to 25 L/m²), respectively. Zahedi et al. (2024) investigated the association between supplemental energy and tank size. They discovered that as tank capacity increases, the average daily auxiliary energy initially declines before increasing again. This tendency is consistent with the patterns presented in Figures 6 and 7, which plot main energy savings ($f_{sav,shc}$) against storage volume. As auxiliary energy declines, PES rise, and vice versa. Similarly, Khan et al. (2018) and Hang and Qu (2010) and El Hassani et al. (2021) observed this tendency in their research, which plotted sun fraction (SF) versus storage amount. They discovered that SF typically peaks at the appropriate storage volume.

Figure 9 and Figure 10 show the seasonal fluctuation in PES ($f_{sav,shc}$) in relation to the needed area of collector for FPC and ETC to meet demands of cooling. Fig. 9 illustrates that the solar cooling absorption system achieves larger $f_{sav,shc}$ as the collector area increases. This effect is more severe for ETCs, especially when the collector area is less than 700 m², as seen in Fig. 9.

Figure 11 depicts the monthly collector efficiencies for the solar system, with collector regions achieving a savings factor ($f_{sav,shc}$) of at least 0.50 (see Fig. 8 and Fig. 9). For this arrangement, the FPC efficiency ranges from 0.16 to 0.219, with an average seasonal efficiency of 0.188. In contrast, the ETC has a substantially greater seasonal efficiency (0.52). The absorption chiller's high driving temperature of 111 °C accounts for the remarkable difference in monthly efficiency between ETC and FPC.

Figure 12 shows the monthly fluctuation in SF from May to September for a 560 m² configuration of ETCs. The SF is larger in May and September because cooling demand is lower during these months than in July, when cooling load is highest. The impact of system setup on SF is negligible, with changes of about 1°. This pattern is similar across collectors from different places, showing that the difference in solar percentage between them is minimal. The SF definition includes periods when the absorption chiller does not always utilize the gathered solar energy (Q_{solar}), especially when the working fluid temperature ($T_{st,o}$) is lower than the required driving temperature (T_{gi}).

Figure 13 and Figure 14 show the anticipated monthly PES for a set collector area of ETC and FPC in a given configuration. The change in solar radiation and cooling demand across the months results in varying primary energy savings. To save 50% on primary energy, a solar absorption system requires a collector area of 400 m². The data in Figs. 12 and 13 show that, for the same collector area, solar systems consistently save more primary energy. The average PES ($f_{sav,shc}$) are larger with a collector area of 400 m².

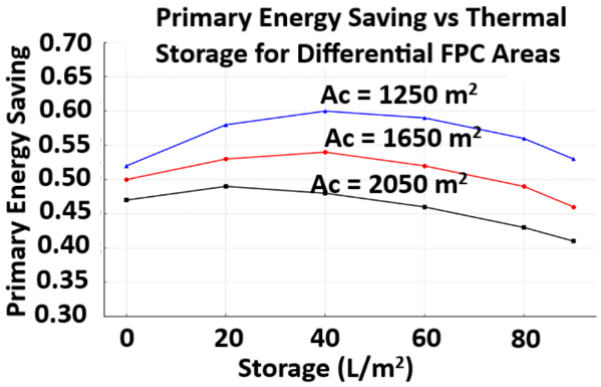

Figure 7: Primary Energy Saving vs. Thermal Storage for Different FPC Areas

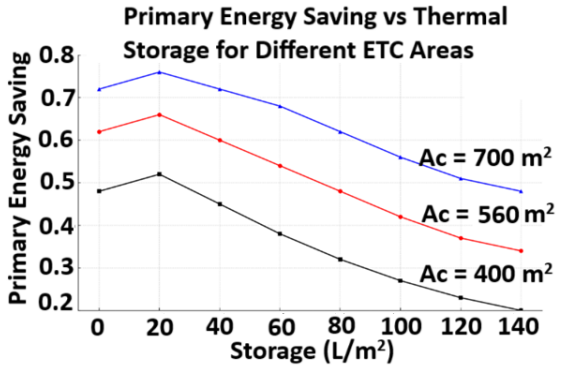

Figure 8: Primary Energy Saving vs. Thermal Storage for Different ETC Areas

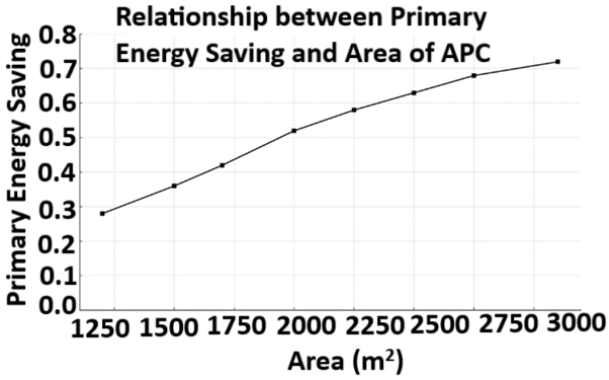

Figure 9: Relationship between Seasonal Primary Energy Saving and Area of FPC

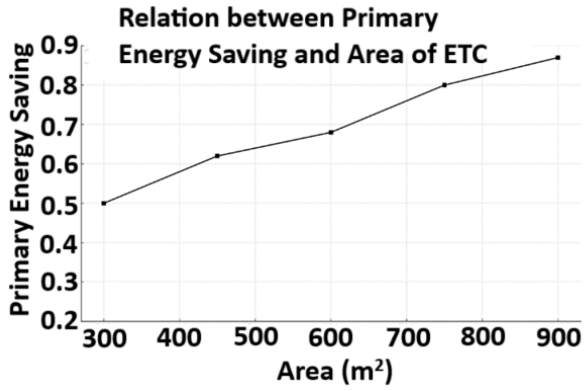

Figure 10: Relationship between Seasonal Primary Energy Saving and Area of ETC

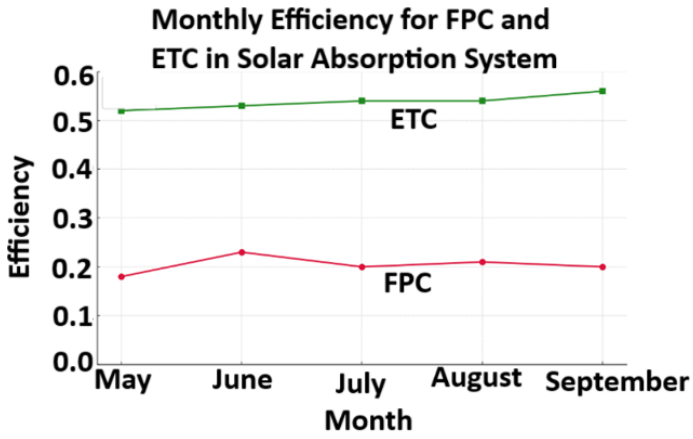

Figure 11: Monthly Efficiency for FPC and ETC in Solar Absorption System

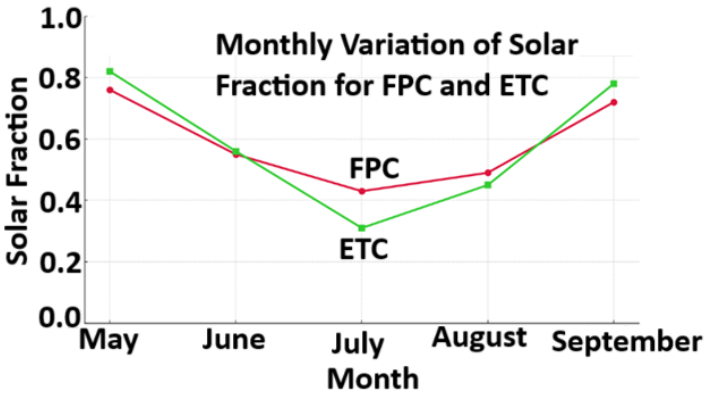

Figure 12: Comparison of Monthly SF between FPC and ETC in a Solar Absorption System

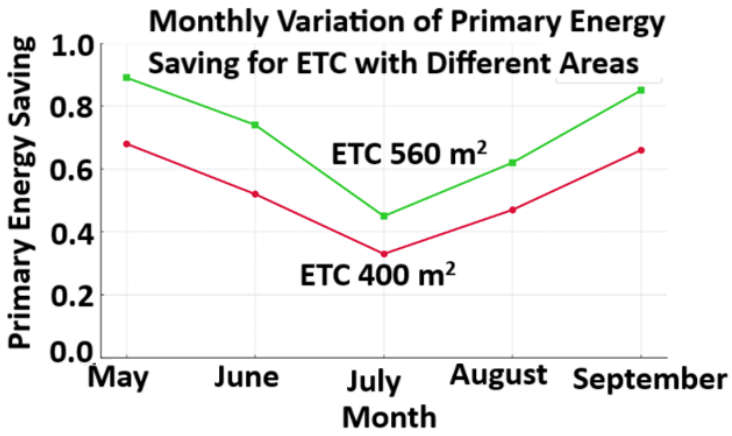

Figure 13: Monthly Variation of PES for ETC with 400 m² and 560 m² Collector Areas

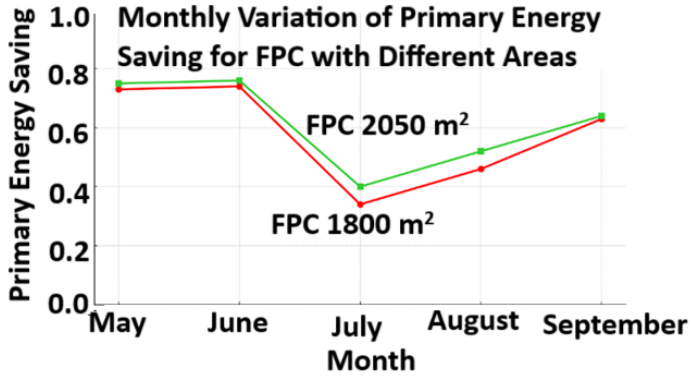

Figure 14: Monthly Variation of PES for FPC with 1800 m² and 2050 m² Areas

3.5. Model Limitations and Future Validation Plans

Although the simulation outcomes align well with trends reported in previous literature, this study lacks direct **quantitative validation using experimental or field performance data**. Several sources of **uncertainty** may affect the accuracy of results:

- **Weather Data Accuracy**: The simulations rely on hourly TMY2 data generated from Meteonorm for Peshawar. While these datasets represent typical meteorological conditions, they do not capture year-to-year variability or short-term extremes, potentially influencing system performance metrics such as peak SF or auxiliary heater engagement.

- **Control Strategy Simplifications**: The control logic in TRNSYS was based on ideal differential temperature thresholds and fixed flow rates. In real systems, control response times, hysteresis effects, sensor inaccuracies, and actuator delays can introduce performance deviations that are not captured in the simulation environment.
- **Component Models and Idealized Behavior**: The TRNSYS component libraries (e.g., Type 700 for auxiliary heaters, Type 4a for stratified tanks) assume consistent operating conditions and do not model transient effects such as scaling, fouling, or degradation over time.
- **Load Profile Representation**: The building cooling load was synthesized using standard occupancy and internal gain assumptions (Type 682). Real buildings exhibit more complex and dynamic thermal behavior due to occupancy patterns, shading, equipment usage, and ventilation.

The key Performance Matrices are given in Table 4

Table 4
Summary of Key Performance Metrics of the Solar-Assisted Absorption Cooling System

Performance Metric	Parameter /Range	Key Observations	Reference Figures
Chilled Water Outlet Temperature	~7°C	Stable and within design range, indicating reliable chiller performance	Fig. 2, Fig. 4
Cooling Water Outlet Temperature	~28°C	Effective heat rejection maintained via cooling tower	Fig. 2, Fig. 4
Hot Water Outlet Temperature	~95°C	Maintained consistently via solar and auxiliary input	Fig. 2, Fig. 3, Fig. 4
Collector Efficiency (ETC)	Average: 0.52	Significantly higher than FPC due to higher operating temperature	Fig. 10
Collector Efficiency (FPC)	Range: 0.16 – 0.219, Avg: 0.188	Lower seasonal efficiency; suitable for moderate temp requirements	Fig. 10
SF of (ETC)	Max: ~0.55 at tilt angle 15°	Peaks in May and September; lower in July due to high cooling demand	Fig. 5, Fig. 11
SF of (FPC)	Max: ~0.49 at tilt angle 15°	Similar pattern as ETC; more area required for similar SF	Fig. 5, Fig. 11
PES (fsav,shc)	Max: 0.50 with ETC (560 m², 14.9 m³); FPC (1650 m², 60 m³)	Peaks with optimal storage volume; increases with collector area, then plateaus or declines	Fig. 6, Fig. 7, Fig. 8, Fig. 9
Auxiliary Energy Behavior	Pulsating pattern, peak flow ≈ 49,000 kg/hr	Operates intermittently; effective in meeting setpoint temperature but may require control optimization	Fig. 3
Optimal Collector Tilt Angle	15°	Yields highest SF under Peshawar summer conditions	Fig. 5
Thermal Storage Volume (Optimal)	ETC: 10–15 m³**,** FPC: 60 m³	Excessive storage leads to reduced efficiency and increased auxiliary energy use	Fig. 6, Fig. 7
Seasonal Performance Variation	Highest savings in May and September	Due to moderate cooling loads; lower SF in peak summer month (July)	Fig. 11, Fig. 12, Fig. 13

A concise and practical design recommendations table based on the simulation results. It highlights optimal configurations for achieving at least 50% PES (fsav,shc ≥

0.50) using either ETC or FPC, along with corresponding tilt angles and storage volumes are shown in Table 5.

Table 5
Design Recommendations for Achieving 50% Primary Energy Savings

Collector Type	Collector Area (m²)	Tilt Angle (°)	Storage Volume (m³)	Storage Ratio (L/m²)	Expected fsav,shc	Key Notes
ETC	400	15	10	25	≥0.50	Most efficient setup; compact system with high thermal performance
ETC	560	15	14.9	27	0.51	Higher margin for energy savings; good for larger cooling demands
FPC	1650	15	60	36	0.50	Requires significantly more area and storage due to lower efficiency

3.6. Policy and Design Implications for Hot-Arid Regions

The integration of solar-assisted cooling systems offers significant potential for peak load reduction in Pakistan's power grid, particularly during summer afternoons when cooling demand is highest. By offsetting grid electricity through solar energy, such systems contribute to peak shaving, reducing the risk of blackouts and easing stress on aging infrastructure. This is especially relevant for urban centers facing frequent load-shedding. Moreover, maintaining thermal comfort during extreme heat events has direct public health benefits, lowering the risk of heat-related illnesses. These findings support the inclusion of solar cooling incentives in national energy policies, encourage the adoption of thermal storage in building codes, and highlight the need for climate-resilient HVAC strategies in future building designs across hot-arid regions.

3.7. Limitations and Future Work

This study is based entirely on simulation using TRNSYS, which, while powerful, cannot fully capture real-world operational uncertainties. The analysis assumes ideal component behavior, constant performance, and perfect maintenance, which may not reflect practical challenges such as degradation, fouling, or control faults. Furthermore, life-cycle cost analysis and environmental impact assessments—such as carbon emissions or embodied energy—were not included and should be addressed in future research. The study also does not account for long-term effects of climate change, such as rising ambient temperatures and solar irradiance variability, which may impact cooling demand and system efficiency over time. Future work should focus on establishing a pilot plant for empirical validation under actual weather and load conditions. Additionally, integrating the system with demand response strategies and incorporating dynamic financial models (e.g., net present value, payback period, and tariff structures) would enhance techno-economic feasibility. Exploring system behavior under projected climate scenarios would also help assess long-term resilience and guide sustainable design in hot-arid regions.

4. Conclusion

This study effectively demonstrates the technical viability and performance optimization potential of a solar-assisted absorption cooling system in Peshawar's hot climate. Simulation results confirm the system's ability to maintain target temperature set points for chilled, cooling, and hot water loops under both steady and dynamic conditions. The auxiliary heater system exhibits high responsiveness, with flow pulsations aligned with solar shortfall events, suggesting effective but aggressive control logic.

Quantitative analysis of SF and PES indicates that a collector tilt angle of 15° maximizes solar input for both FPC and ETC configurations. Notably, ETCs outperformed

FPCs, achieving $f_{sav,shc} \geq 0.49$ with a reduced collector area (400–560 m²) and optimized storage volume of approximately 25 L/m². Thermal storage capacity significantly influences system performance, where oversizing beyond the optimal range diminishes energy savings due to increased auxiliary load.

Seasonal cooling loads exhibited significant variability, emphasizing the importance of adaptive control and potential integration of thermal buffering or predictive cooling strategies. The collector efficiency data confirmed that ETCs are far more suitable for high-temperature absorption cooling, achieving nearly triple the efficiency of FPCs.

The conclusions drawn in this study are based on simulations using TMY2 weather data specific to Peshawar, which reflect long-term seasonal and diurnal climate trends. This ensures that the system sizing, operational strategies, and performance outcomes are locally relevant and robust. The close alignment between simulation profiles and actual climatic conditions in the region supports the practical applicability of the design recommendations. For further validation, future work may include comparisons with real-time field data to enhance the accuracy and reliability of the proposed system.

The findings of this study have important practical and policy implications for addressing Pakistan's rising cooling demand. The recommended system configurations can inform building energy codes and support sustainable design in public infrastructure. Although a detailed cost analysis was not included, the proposed system—using ETCs and moderate storage—appears economically feasible in the long term, especially with government incentives. There is potential for local manufacturing of solar thermal components, which could reduce costs and create jobs. To encourage adoption, policy measures such as tax relief, import duty reductions, or performance-based subsidies are recommended. Integrating solar cooling into national energy and climate strategies can help reduce peak loads and support Pakistan's sustainability goals.

Based on the findings, engineers are encouraged to adopt ETC-based solar cooling systems with optimized sizing for high-efficiency applications. Building owners should consider these systems as sustainable alternatives for reducing operational energy costs. Government agencies are advised to support adoption through targeted incentives and integration into building codes. Future work should focus on pilot-scale implementation, detailed cost-benefit analyses, and scaling the system design to other regions in Pakistan or countries with similar climatic conditions.

Acknowledgement

I would like to express my sincere gratitude to the Energy Center, University of Engineering and Technology (UET), Peshawar, for providing access to the TRNSYS 18 simulation software, which played a pivotal role in the successful completion of this study. The availability of this advanced tool enabled accurate modeling and analysis of the energy systems considered in this project. I deeply appreciate their support and commitment to promoting research and innovation in the field of sustainable energy.

Authors Contribution

Abid Hussain: Research Paper original draft writing, TRNSYS Analysis.
Asnaf Aziz: Conducted data collection related to solar radiation and local climate conditions in Peshawar and assisted in model calibration.
Afzal Khan: Supervision, Review and editing of the paper.
Nadeem Ur Rehman: Performed the performance analysis and validation of simulation results with reference data.
Hamza Parvez: Contributed to literature review, structured the manuscript, and prepared the figures and tables.
Altaf Husain: Handled the final editing, formatting, referencing using zotero, and ensured compliance with journal submission guidelines. Analysis

Conflict of Interests/Disclosures

The authors declared no potential conflicts of interest w.r.t. the research, authorship and/or publication of this article.

References

Asim, M. (2016). *Simulation of solar powered absorption cooling system for buildings in Pakistan*: The University of Manchester (United Kingdom).

Assilzadeh, F., Kalogirou, S. A., Ali, Y., & Sopian, K. (2005). Simulation and optimization of a LiBr solar absorption cooling system with evacuated tube collectors. *Renewable energy, 30*(8), 1143-1159. doi:https://doi.org/10.1016/j.renene.2004.09.017

Bhatkar, V. W., Kriplani, V., & Awari, G. (2013). Alternative refrigerants in vapour compression refrigeration cycle for sustainable environment: a review of recent research. *International Journal of Environmental Science and Technology, 10*(4), 871-880. doi:10.1007/s13762-013-0202-7

Darema, F. (2005). *Dynamic data driven applications systems: New capabilities for application simulations and measurements.* Paper presented at the International conference on computational science.

El Hassani, S., Charai, M., Moussaoui, M. A., & Mezrhab, A. (2021). *Simulation of a solar driven air conditioning system for mitigating the cooling demand of buildings located in semi-arid climates: A case study.* Paper presented at the International Conference Interdisciplinarity in Engineering.

Gang, W., Wang, S., Xiao, F., & Gao, D.-c. (2016). District cooling systems: Technology integration, system optimization, challenges and opportunities for applications. *Renewable and Sustainable Energy Reviews, 53*, 253-264.

Hang, Y., & Qu, M. (2010). The impact of hot and cold storages on a solar absorption cooling system for an office building.

Hays, R. T., & Singer, M. J. (2012). *Simulation fidelity in training system design: Bridging the gap between reality and training*: Springer Science & Business Media.

Khan, M. S. A., Badar, A. W., Talha, T., Khan, M. W., & Butt, F. S. (2018). Configuration based modeling and performance analysis of single effect solar absorption cooling system in TRNSYS. *Energy conversion and management, 157*, 351-363. doi:https://doi.org/10.1016/j.enconman.2017.12.024

Klein, S. A. (1988). TRNSYS-A transient system simulation program. *University of Wisconsin-Madison, Engineering Experiment Station Report*, 38-12.

Perwez, U., Sohail, A., Hassan, S. F., & Zia, U. (2015). The long-term forecast of Pakistan's electricity supply and demand: An application of long range energy alternatives planning. *Energy, 93*, 2423-2435. doi:https://doi.org/10.1016/j.energy.2015.10.103

Ren, J., Qian, Z., Yao, Z., Gan, N., & Zhang, Y. (2019). Thermodynamic evaluation of LiCl-H2O and LiBr-H2O absorption refrigeration systems based on a novel model and algorithm. *Energies, 12*(15), 3037. doi:https://doi.org/10.3390/en12153037

Rojas, D., Beermann, J., Klein, S., & Reindl, D. (2008). Thermal performance testing of flat-plate collectors. *Solar Energy, 82*(8), 746-757. doi:https://doi.org/10.1016/j.solener.2008.02.001

Shesho, I. (2014). *Analysis and design of solar based systems for heating and cooling of buildings.* Institutt for energi-og prosessteknikk,

Tress, W., Domanski, K., Carlsen, B., Agarwalla, A., Alharbi, E. A., Graetzel, M., & Hagfeldt, A. (2019). Performance of perovskite solar cells under simulated temperature-illumination real-world operating conditions. *Nature energy, 4*(7), 568-574.

Zahedi, R., Shaghaghi, A., Aslani, A., Noorollahi, Y., Razi Astaraei, F., & Eskandarpanah, R. (2024). Optimization of a hybrid cooling, heating and power multigeneration system coupled with heat storage tank using a developed algorithm. *Journal of Thermal Analysis and Calorimetry, 149*(19), 11107-11117.